

Backward angle cross sections for $^{27}\text{Al}+^{16}\text{O}$ reaction products

D. Shapira, J. L. C. Ford, Jr., J. Gomez del Campo, and P. H. Stelson

Oak Ridge National Laboratory, Oak Ridge, Tennessee 37830

(Received 10 December 1979)

Reactions induced by bombarding a ^{16}O gas target with ^{27}Al ions were studied. Evaporation residues as well as target-like recoils were measured over a wide range of Q values. The yield of particles with $6 \leq Z \leq 9$ was found to be forward peaked in the laboratory frame. These target-like particles emerge with center-of-mass kinetic energies that, on the average, are independent of the reaction angle. Their combined cross section has a $1/\sin\theta_{\text{c.m.}}$ angular dependence. If this cross section is assumed to be symmetric about 90° (c.m.) the integrated cross section is about 10% of the measured evaporation residue cross section at a center-of-mass energy of 54 MeV.

NUCLEAR REACTIONS $^{27}\text{Al}+^{16}\text{O}$, $E_{^{27}\text{Al}} = 105, 145$ MeV; measured $d\sigma/d\Omega$ for reaction products with $6 \leq Z \leq 9$ and $Z > 13$ for $2.5^\circ \leq \theta_L \leq 15^\circ$. Extracted σ for evaporation residues and damped events.

I. INTRODUCTION

The $^{16}\text{O}+^{27}\text{Al}$ system has been the subject of numerous studies.¹⁻⁵ The evaporation residue cross sections have been measured by bombarding ^{27}Al targets with ^{16}O beams at many different bombarding energies,^{1,3,4} and some features have emerged that set it apart from other systems with similar mass. The resulting energy dependence, when analyzed in the framework suggested by Glas and Mosel,⁶ yields values for the critical radius and critical potential¹ ($r_{\text{cr}} = 0.79$ fm and $V_{\text{cr}} = -40$ MeV) which deviate significantly from the values one would expect on the basis of systematic trends in this mass region ($r_{\text{cr}} = 1.0$ to 1.1 fm and $V_{\text{cr}} \sim 0$ MeV).⁷ Furthermore, a large component of strongly damped events with masses and charges near that of the beam (^{16}O) has been observed.² These events are forward peaked and have been identified² as deep inelastic reaction products.

In the present measurements on the $^{16}\text{O}+^{27}\text{Al}$ system the target and projectile were interchanged. By having the lighter particle as the target, we were able to simultaneously detect evaporation residues as well as the forward scattered target-like particles. Use of a gas target of ^{16}O enabled the identification of reaction processes over a wide range of energy loss, mass, and Z without the confusion often due to light contaminants. In this measurement we detected strongly damped-target-like products at forward angles. In this way we were able to extend the earlier measurements of damped events, done with ^{16}O as the beam, to the backward hemisphere. The angular distribution measured for these "deep inelastic" events shows a backward angle rise and

follows on the average a $1/\sin\theta_{\text{c.m.}}$ angular distribution in the backward hemisphere.

II. EXPERIMENTAL PROCEDURE AND RESULTS

A natural oxygen gas target⁸ was bombarded with 120- and 160-MeV ^{27}Al beams from the Brookhaven National Laboratory MP tandem accelerator. The experimental setup is shown in Fig. 1. The beam was tightly collimated by two slits, C_1 and C_2 , which were about one meter apart. The target cell was constructed in a way that allowed simultaneous measurement of reaction products emerging on both sides of the beam. By detecting reaction products on both sides of the beam it was possible to monitor the average position and angle of incidence of the beam. The reaction products were identified using two ΔE - E counter telescopes. A gas ionization chamber backed by a solid state detector⁹ provided energy loss and residual energy signals for each event. The solid angles of both detectors were determined from the measured dimensions by geometric calculations⁸ and with a calibrated α -particle source. The absolute norm-

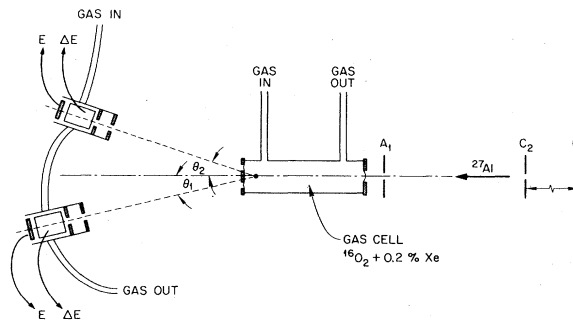


FIG. 1. A schematic of the experimental setup.

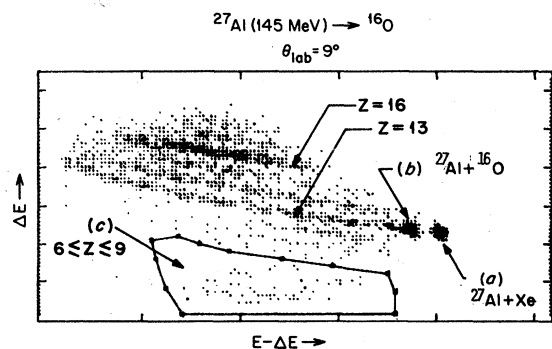


FIG. 2. A two-dimensional spectrum for $^{27}\text{Al}+^{16}\text{O}$ reaction products. (a) is the peak corresponding to $^{27}\text{Al}+\text{Xe}$ elastic scattering. (b) is the $^{27}\text{Al}+^{16}\text{O}$ elastic scattering peak. (c) damped-target-like events.

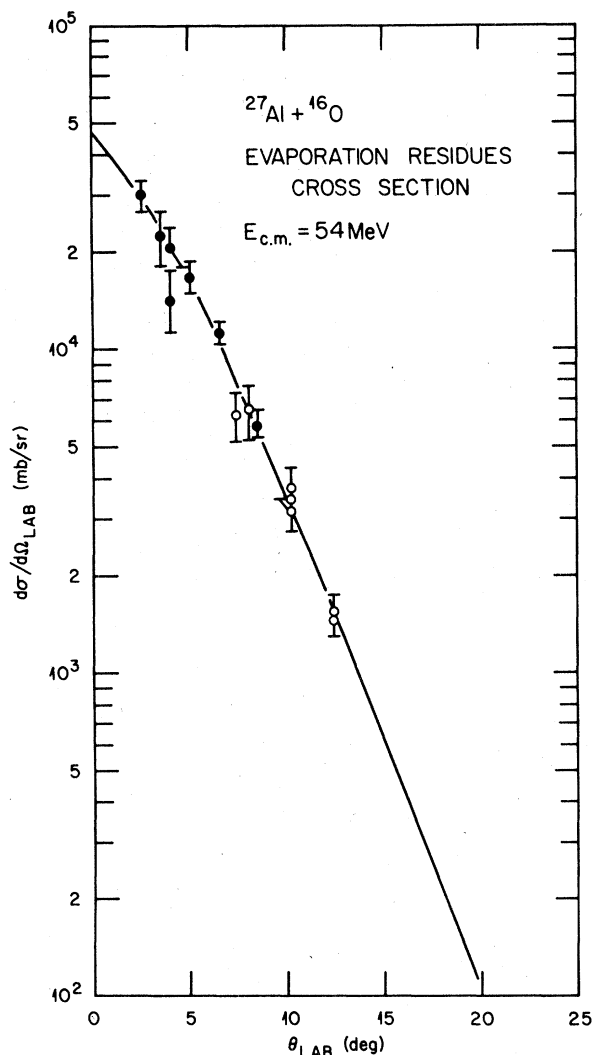


FIG. 3. Angular distribution for evaporation residues measured at a center-of-mass energy of 54 MeV. The open and closed circles correspond to measurements on opposite sides of the beam (see Fig. 1).

alization of the data was obtained from scattering of the ^{27}Al beam by Xe gas mixed with the target gas at a $0.2\% \pm 0.004\%$ molar ratio. More details on the geometric corrections and normalization procedure are available from Ref. 8. A typical two-dimensional E vs ΔE spectrum is shown in Fig. 2. The two elastic peaks resulting from $^{16}\text{O}+^{27}\text{Al}$ and $\text{Xe}+^{27}\text{Al}$ elastic scattering are indicated, as is the two-dimensional gate drawn around the events which we designate as recoiling target-like nuclei ($Z \sim 8$). The evaporation residues are clustered around the strong $Z = 16$ line located above the ^{27}Al line. At more forward angles the yield from evaporation residues became much more intense and was shifted toward higher Z values. Measurements were performed at eleven angles spanning 2.5° to 15° in the laboratory system. Figure 3 displays an angular distribution for evaporation residues with $Z > 13$ measured at $E_{\text{c.m.}} = 54$ MeV.¹⁰ The resulting integrated evaporation residue cross section is 1260 ± 220 mb. A comparison was made with mass and charge distributions from previous measurements at similar energies¹⁻³ and with the elemental distributions predicted by a Hauser-Feshbach multiparticle evaporation code.¹¹ As a result, we believe that by summing evaporation residues with $Z > 13$ we obtain more than 96% of the total evaporation residue yield. The large uncertainties are mainly a result of low counting statistics in the $\text{Xe}+^{27}\text{Al}$ elastic scattering peak.

We now focus our attention on the reaction products encircled by the two-dimensional mask shown

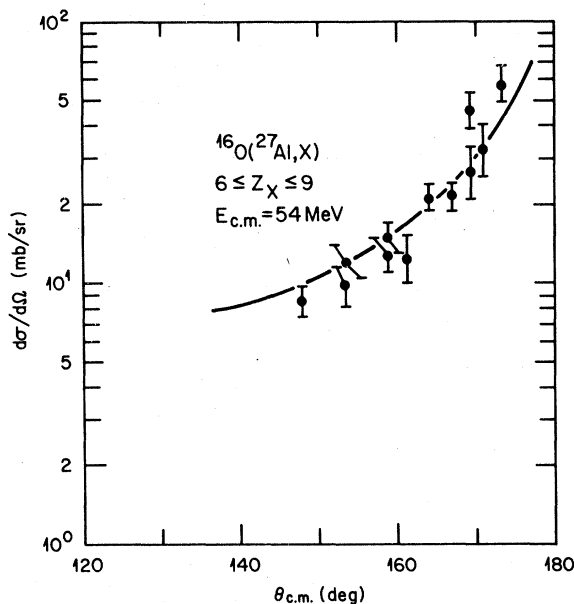


FIG. 4. Center-of-mass angular distribution for damped events at large angles and $E_{\text{c.m.}} = 54$ MeV.

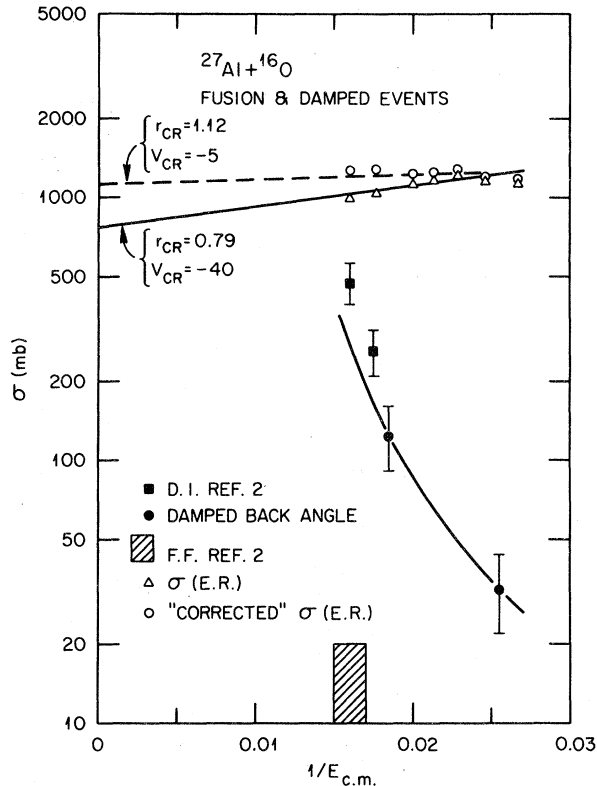


FIG. 5. Evaporation residue cross sections from Ref. 1 are shown by triangles; the open circles are the same but corrected for fission (see text). Damped back angle cross sections due to $^{27}\text{Al}+^{16}\text{O}$ collisions are shown by solid circles. Also shown are the damped events identified as deep inelastic scattering in Ref. 2 (solid squares). The error bars are not shown for the fusion and the evaporation residue cross sections. The uncertainties are the same as given in Ref. 2. The shaded bar indicates the upper limit on fusion-fission events suggested in Ref. 2. The hyperbolic curve drawn through our data points for damped events at backward angles corresponds to an exponential energy dependence.

in Fig. 2. Assuming two-body kinematics, it was found that events with $6 \leq Z \leq 9$ could be associated with a range of Q values whose average is approximately the same at all angles studied, ($6^\circ \leq \theta_{c.m.} \leq 40^\circ$); $\bar{Q} = -22$ and -32 MeV for $E_{c.m.} = 39$ and 54 MeV. Using the average Q value for all the events in this group yields the center-of-mass angular distribution shown in Fig. 4. The solid curve is proportional to $1/\sin\theta_{c.m.}$. Assuming that the angular distribution for this process is symmetric about 90° , the total cross section for these events can be obtained (120 ± 25 mb at 54 MeV, Fig. 4). The total cross section deduced for this process, at the two energies studied, is shown in Fig. 5 (the solid circles). Also appearing in the same plot are the assigned total deep inelastic cross sections quoted in Ref. 2. While the present

data and those of Ref. 2 were measured at slightly different energies, it is interesting to note that their cross sections lie close to the extrapolated curve through our data.

III. DISCUSSION

Our measurements show the presence of strongly damped-target-like events which have a $1/\sin\theta_{c.m.}$ angular distribution in the backward hemisphere. These events have Q values and Z distributions which are similar to those reported as deep inelastic scattering by Cormier *et al.*² at slightly higher energies and at scattering angles in the forward hemisphere. The angular distribution in Fig. 4 shows that the present data are due to a mechanism having a long interaction time; however, the degree of equilibration of the composite system is yet an open question.

The yield observed here could be the backward angle part of the deep inelastic process previously observed at forward angles.² One can view, then, the $1/\sin\theta_{c.m.}$ angular distribution in the backward hemisphere as yet another confirmation that deep inelastic scattering is an orbiting phenomenon.¹²⁻¹⁴ The relaxed events seen here could originate also from a completely equilibrated system. The factor limiting large fragment emission could be the level density at the saddle-point configuration,¹⁵ or the phase space available for the two fragments at infinite separation.¹⁶ Estimating the fission with the code ALICE¹⁷ results in very low $\Gamma_{\text{fission}}/\Gamma_{\text{total}}$ values. No attempt has been made to estimate the rate of large fragment evaporation using the second approach mentioned above, since for such a calculation the excitation energy and spin of both outgoing fragments has to be taken into account and such a code does not yet exist. It should be noted, however, that a 10% fission yield due to fission evaporation competition would be surprisingly large for a compound nucleus with mass number 42 and excitation energy of 70 MeV.¹⁸

One possible means of determining the degree of equilibration is to measure the full angular distribution. Symmetry about 90° would indicate that the events originate from a fusion-fission process. Unfortunately, the counting statistics of the data observed in our forward angle counters is inadequate to obtain meaningful separation of strongly damped and quasi-elastic cross sections at these angles. A comparison with the results obtained by Cormier *et al.*² is also difficult because our data were measured at slightly lower energies and these cross sections depend very strongly on energy (Fig. 5). However, the upper limit placed on fusion-fission events in Ref. 2 (where presumably only symmetric fission was considered) is much lower than the trend indicated by our data (see

Fig. 5).

Although it is still an open question as to whether the oxygen-like damped events observed in the present experiment originate from fusion-fission or orbiting, it is interesting to examine the consequences of an assumed fusion-fission process. If this were indeed the reaction mechanism producing these damped-target-like products, then the measured evaporation residue cross section would no longer account for the entire fusion cross section. In this case, the fusion-fission contribution must also be added to the evaporation residue cross section. The evaporation residue cross sections of Ref. 1 (open triangles in Fig. 5) "corrected" in this manner, are indicated by the open circles in the figure. The anomalous behavior reported for the $^{27}\text{Al}+^{16}\text{O}$ system¹ compared to the systematic trend of fusion cross sections for light systems then disappears; the new r_{cr} and

V_{cr} values extracted are 1.1 fm and 5 MeV, respectively.

In conclusion, our data show the presence of a pronounced backward angle yield of strongly damped events, with an angular distribution characteristic of a long interaction time. However, the degree of equilibration of the composite system that produces this yield remains uncertain.

ACKNOWLEDGMENTS

We thank G. Hummer of BNL for his help throughout the experiment. Discussions with and critical comments by R. G. Stokstad and F. Plasil are gratefully acknowledged. This research was supported by the Department of Energy under Contract No. W-7405-eng-26 with Union Carbide Corporation.

¹B. B. Back, R. R. Betts, C. Gaarde, J. S. Larson, E. Michelson, and Tai Kuang-Hsi, Nucl. Phys. A285, 317 (1977).

²T. M. Cormier, A. J. Lazzarini, M. A. Neuhausen, A. Sperduto, K. Van-Bibber, F. Videback, G. Young, E. B. Blum, L. Herreid, and W. Thoms, Phys. Rev. C 13, 682 (1976).

³R. L. Kozub, N. H. Lu, J. M. Miller, D. Logan, T. W. Debiak, and L. Kowalski, Phys. Rev. C 11, 1497 (1975).

⁴Y. Eisen, I. Tserruya, Y. Eyal, Z. Fraenkel, and M. Hillman, Nucl. Phys. A291, 459 (1977).

⁵J. Dauk, K. P. Lieb, and A. M. Kleinfeld, Nucl. Phys. A241, 270 (1975).

⁶D. Glas and U. Mosel, Nucl. Phys. A275, 429 (1975).

⁷D. Horn, A. J. Ferguson, and O. Hausser, Nucl. Phys. A311, 238 (1978).

⁸D. Shapira, R. Dayras, J. L. C. Ford, Jr., J. Gomez del Campo, A. H. Snell, P. H. Stelson, and R. G. Stokstad, Nucl. Instrum. Methods 163, 325 (1979).

⁹We thank J. Barrette and C. Thorn for providing the two detector systems.

¹⁰The center-of-mass energy quoted here already takes

into account the energy lost by the projectile in the target gas cell. The resulting uncertainty in energy is ± 1 MeV in the center of mass.

¹¹LILITA, a Hauser-Feshbach Monte Carlo Evaporation Code, J. Gomez del Campo and R. G. Stokstad.

¹²D. Shapira, J. L. C. Ford, Jr., J. Gomez del Campo, R. G. Stokstad, and R. M. DeVries, Phys. Rev. Lett. 43, 1781 (1979).

¹³J. Wylcinski, Phys. Lett. 47B, 484 (1973).

¹⁴P. Dyer, R. J. Puigh, R. Vandenbosch, T. D. Thomas, and M. S. Zisman, Phys. Rev. Lett. 39, 392 (1977); W. Trautman, J. de Boer, W. Dunnweber, G. Graw, R. Kopp, C. Lauterbach, H. Puchta, and U. Lynen, *ibid.* 39, 1062 (1977).

¹⁵F. Plasil and M. Blann, Phys. Rev. C 11, 5081 (1973).

¹⁶L. G. Moretto, Nucl. Phys. A247, 211 (1975).

¹⁷F. Plasil, ORNL ALICE, Oak Ridge National Laboratory Report No. ORNL/TM-6054.

¹⁸C. K. Gelbke, P. Braun-Munzinger, J. Barrette, B. Zeidman, M. J. Levine, A. Gamp, H. L. Harney, and Th. Walcher, Nucl. Phys. A269, 460 (1976) and references therein.